

COB-2023-0654

EXPERIMENTAL STUDY OF GAS-LIQUID FLOW THROUGH AN ORIFICE PLATE USING HIGH SPEED CAMERA AND DIFFERENTIAL PRESSURE MEASUREMENT

Josiane Weise
Rafael F. L. de Cerqueira
Emilio E. Paladino

SINMEC - Computational Fluid Dynamics Lab, Mechanical Engineering Department, Federal University of Santa Catarina, 88040-900 - Florianópolis - SC, Brazil
josiane.weise@gmail.com
rafael.cerqueira@ufsc.br
emilio.paladino@ufsc.br

Abstract. Differential-pressure (DP) flow meters are widely used as a part of the systems designed for multiphase flow rate measurement without prior phase separation due to their characteristics of simplicity and robustness. For multiphase flows with high gas volume fraction (wet gas flow), a common approach is to measure the gas flow rate from the multiphase DP through the throttle device combined with an over-reading (OR) correlation. This correlation corrects the positive deviation in the measurement due to the liquid content. Therefore, the liquid phase fraction is an input parameter in the OR correlations and the throttle device should be associated with some technique dedicated to phase fraction evaluation to allow inline multiphase flow rate measurement. A method proposed in the literature is the determination of the phase fraction from its correlation with statistical parameters of the DP signal fluctuations, usually based on the DP standard deviation. In this way, gas and liquid mass flow rates can be measured by one throttle device, considering the mean and fluctuations of the DP signal. The main purpose of this work is to investigate the relationship between the flow structure and transient DP signal of gas-liquid flows with high gas volume fraction and high gas superficial velocity to provide proper physical support for the correlation between the fluctuations of the DP signal and the liquid phase fraction. The experimental investigation was developed analyzing images captured from a High-Speed Camera (HSC) and measuring the DP signal in high gas content gas-liquid flow through an orifice plate. The experimental apparatus comprises a horizontal acrylic section with an internal diameter (D) of 25.4 mm. The orifice plate with a diameter ratio of 0.5 was installed at $100 D$ from the inlet. A set of superficial velocities of gas and liquid was evaluated, all within the region of stratified and wavy flow patterns. The HSC and the DP sensor were synchronized, allowing for the correlation between the observed flow structure and the DP signal. Liquid film height in the images was also determined from image processing techniques. The DP fluctuations depend mainly on the characteristics of the waves in the upstream flow of the orifice plate. Waves propagation through the orifice plate causes a significant decrease in the gas flow area, promoting large amplitude fluctuations in the DP signal. As the characteristics of the waves are fundamentally dependent on the gas and liquid superficial velocities, the results clarify the basis of the correlation between the liquid fraction and DP fluctuations in the range of conditions analyzed.

Keywords: inline two-phase flow metering, orifice plate, transient two-phase flow, differential pressure fluctuation, gas-liquid flow visualization

1. INTRODUCTION

Multiphase flow rate measurement without prior phase separation requires the evaluation of more than one flow variable. Differential-pressure (DP) flow meters are usually an essential part of these systems designed for inline multiphase flow measurement, especially in applications with low liquid loading, like in wet gas flow conditions. Regardless of the amount of liquid, the DP through the throttle device for a two-phase flow is higher than the DP that would be observed for a single-phase gas flow with the same mass flow rate. A common practice for two-phase flow measurement with DP devices considering flows with high gas volume fraction is to estimate the gas mass flow rate from the mass and energy balances from the multiphase DP (ΔP_{tp}). Then an over-reading (OR) correction is applied to determine the actual gas mass flow rate, such that

$$m_g = \frac{C_d \varepsilon A_0 (1 - \beta^4)^{-0.5} (2\rho_g \Delta P_{tp})^{0.5}}{OR}, \quad (1)$$

where C_d is the discharge coefficient, ε is the expansibility coefficient, A_0 is the throat cross-sectional area, β is the

diameter ratio, and ρ_g is the gas density. Two classical OR correlations were proposed by Murdock (1962) and Chisholm (1977), which are presented, respectively, in Eq. 2 and Eq. 3,

$$OR = 1 + 1.26X_{LM}, \quad (2)$$

$$OR = (1 + C_{Ch}X_{LM} + X_{LM}^2)^{0.5}, \quad (3)$$

where

$$C_{Ch} = (\rho_g/\rho_l)^{0.25} + (\rho_g/\rho_l)^{-0.25}. \quad (4)$$

X_{LM} in Eq. 2 and Eq. 3 is the Lockhart-Martinelli parameter, given by,

$$X_{LM} = \frac{1-x}{x} \sqrt{\frac{\rho_g}{\rho_l}}, \quad (5)$$

where x is the dynamic gas mass fraction and ρ_l is the liquid density. Several other OR correlations are presented in the literature (Lin, 1982; Steven, 2002; Pan *et al.*, 2019). Similarly, a two-phase mass flow coefficient can be used to correct the measurement of the two-phase mass flow rate (He and Bai, 2014).

The main challenge related to using the OR correlations, or two-phase mass flow coefficients, is that the liquid flowrate or the liquid fraction needs to be known before the measurement, which is difficult in practical applications (Li *et al.*, 2020b). An alternative method that has been investigated by some researchers is based on the correlation between the liquid fraction and DP signal fluctuations. In this way, with a single DP flow meter, the average pressure drop along the throttle device is correlated with the gas or total mass flow rate, and the fluctuations of the DP signal are used to determine the liquid fraction. This method has a low implementation cost and avoids using methods specifically designed for phase fraction measurement, which are usually more complex and not suitable for direct application in industry, especially in the oil and gas segment.

In this context, Wenran and Yunxian (1995) related the statistical variance of the DP square root in orifice plates with the mass flow of the liquid phase from theoretical models and experiments. Xu *et al.* (2003) also demonstrated a correlation between the relative fluctuation of the DP signal and wet gas quality from data obtained in a Venturi meter. Zheng *et al.* (2016) analyzed flow through an orifice plate and showed an exponential correlation between the mean square deviation of the DP signal and the gas mass fraction. The transient responses of DP signals have also been used in conjunction with machine learning techniques for inline flow measurement of multiphase flows (Li *et al.*, 2020a). From these studies, remarkably, the correlation between the liquid fraction with parameters related to DP fluctuations has great potential for application in the industry. However, the studies in the literature focus on fitting a correlation usually between the ratio of standard deviation and the mean of the DP signal with the liquid fraction without addressing the fluid dynamics that characterize this correlation.

To better understand the interaction of the two-phase flow structure and the DP flow meter, some techniques for void fraction measurement based on conductive probes and capacitive sensors have been used, as well as the acquisition of flow images. Regarding experiments conducted with orifice plates, Maidana and Rosa (2018) investigated flow disturbances induced by an orifice plate with different diameter ratios in a horizontal air-water flow in the slug pattern for a liquid superficial velocity of 0.3 m/s and gas superficial velocity of 0.5 m/s. They measured instantaneous DP through the orifice plate and the void fraction by single-wire conductive probes, and flow visualization was also performed. Spectral analysis revealed a correspondence between the frequency of passage of slugs through the orifice and the frequency of orifice pressure fluctuations. Ma *et al.* (2020) performed a visualization experiment to study the effects of gas superficial velocity (0.07 to 0.51 m/s), liquid superficial velocity (0.35 to 1.77 m/s), and orifice plate diameter ratio (0.30 to 0.61) in flow pattern transition downstream of single-orifice plates. Almalki and Ahmed (2020) developed a multichannel void fraction sensor to investigate the effect of orifice plates on flow pattern development, evaluating four area ratios. Instantaneous void fraction measurements were obtained at various locations upstream and downstream of the restriction. In addition, pressure measurements and flow visualizations were performed to investigate the dynamic characteristics of flow through the orifice. Liquid superficial velocities of 0.526 and 1.08 m/s and gas superficial velocities ranging from 0.164 to 2.795 m/s were selected to represent the intermittent flow pattern. As can be noted, all of these studies were performed at low liquid superficial velocities, and only in the work of Maidana and Rosa (2018) the relation between flow structure and DP fluctuations is mentioned.

In addition to evaluating conditions with higher gas superficial velocities compared to the works referenced, in this work, image processing techniques are used to characterize the liquid film height upstream of the orifice plate. Different two-phase gas-liquid flow patterns have been studied using image processing techniques. In slug flows, the studies focus on obtaining the size, velocity, and frequency of Taylor bubbles (do Amaral *et al.*, 2013; Widyatama *et al.*, 2018). For stratified wavy flow, the wave characteristics and dynamic properties have been evaluated by image processing techniques. In this context, Ayati *et al.* (2017) characterized the interfacial waves in operational conditions close to the transition between smooth stratified flow and wavy-stratified flow within the linear regime of development of the waves. Kuntoro

et al. (2016) presented improvements in an algorithm previously developed by the authors for image processing, capable of determining the measurements of the film height and the geometric characteristics of waves in stratified flows. Hudaya *et al.* (2019) experimentally analyzed the wavy stratified flow for a range of superficial velocities between 4 m/s and 16 m/s for air and 0.02 m/s and 0.075 m/s for water in a 26 mm constant internal diameter pipe. From the images, the authors determined the frequency, velocity, amplitude, and length of the waves.

The experimental analysis conducted in the present work aims to study the gas-liquid flow in a wavy-stratified pattern through an orifice plate, considering the lack in the literature about: (i) the correlation between the transient structures of the flow with the DP fluctuations and (ii) flow visualization studies of gas-liquid flows with high gas volume fraction through orifice plates. The acquisition of the images was performed in a synchronized way with the DP signal, and the transient fluctuations of the liquid height upstream of the orifice plate were obtained using image processing techniques. With a better understanding of how DP fluctuations are related to the liquid fraction in the flow, it is expected to contribute to the development of the method in which the gas and liquid flow rates can be obtained from a single DP meter.

2. MATERIAL AND METHODS

2.1 Experimental facility and operating conditions

The experimental apparatus is schematically depicted in Fig. 1a. The test section is made in acrylic and has an internal diameter (D) of 25.4 mm and a total length of $160D$. The orifice plate is located $100D$ from the inlet and consists of a 3 mm thick acrylic disk with a diameter ratio of 0.5. Pressure taps are located at a distance of $1D$ from the upstream and downstream of the orifice plate faces. To avoid image distortion due to the curvature of the pipe, the flow visualization section was built following the model of the visualization section presented in Maidana (2017) and it consists of two rectangular acrylic blocks with a central machined hole with the same internal diameter of the pipe. The two blocks are joined with the orifice plate between them.

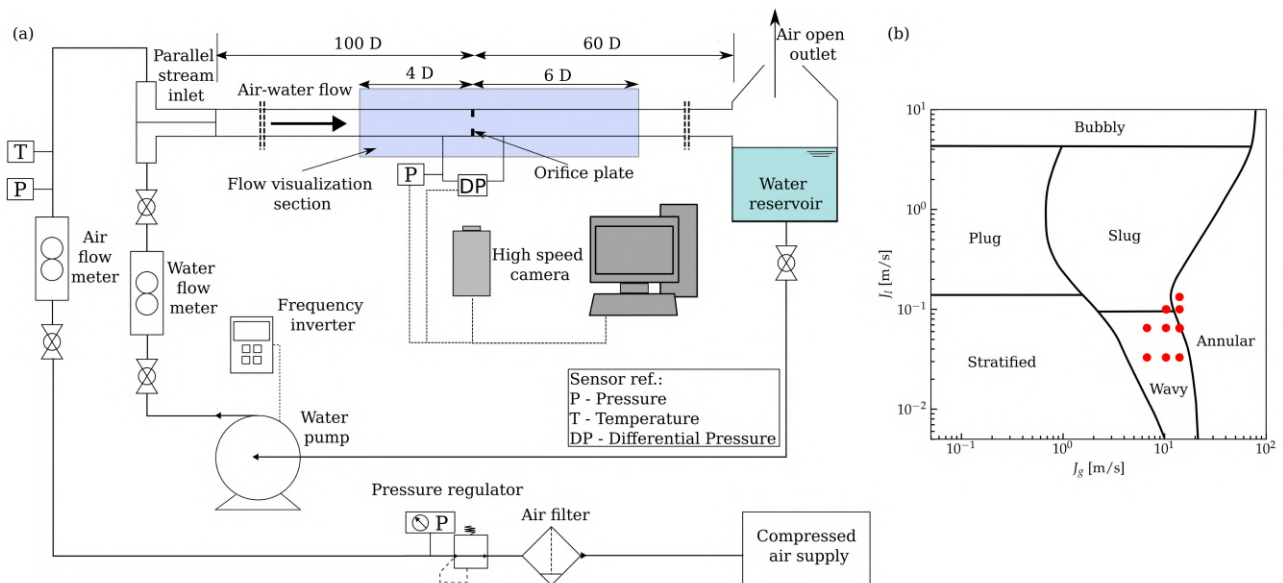


Figure 1. (a) Schematic of the experimental setup and (b) gas and liquid superficial velocities of the experimental conditions shown on the Mandhane *et al.* (1974) flow pattern map.

Experiments were carried out at room temperature and low pressure, close to the atmospheric condition. The air and water are injected respectively at the top and bottom of an inlet device, allowing both phases to flow initially parallel to each other. The main compressed air line supplies the air, and the water is recirculated through the circuit by a centrifugal pump. The air-water mixture is discharged into an open reservoir placed at the end of the test section, where the air vents into the atmosphere.

The air line pressure is adjusted by a pressure regulator to obtain the desired gas flow rate in each operational condition evaluated. The volumetric gas flow rate is measured by an OMEGA FL-2095 rotameter, with a range of 100 to 1,400 standard l/min with $\pm 2\%$ full-scale accuracy. Pressure and temperature sensors were installed downstream of the rotameter to determine the actual gas flow rate at the measured condition. The water flow rate is measured by an OMEGA FL-46303 rotameter flow meter with a range of 1.00-7.50 l/min with $\pm 5.0\%$ full-scale accuracy. A SMAR LD301 DP transmitter with a range of 4.15-500 mBar is used for DP measurement in the orifice plate, with $\pm 0.075\%$ span accuracy. A pressure transducer is also connected to the upstream tap of the DP sensor for local pressure reference.

The analog signals from the transducers are sampled at 1 kHz and converted in the multifunctional data acquisition device NI USB-6002 from National Instrument. The flow images were obtained from a CCD digital High-Speed Camera (Redlake MotionPro X3) using the Motion Studio software from IDT. For each experimental condition, 3,200 images were recorded with a frame rate of 500 fps. The method of camera triggering from a voltage pulse was used to allow synchronization between the image acquisition from the HSC and the acquisition of DP signal. The pulse was controlled by the acquisition device USB-6002. An additional circuit that includes a photoresistive sensor (LDR) coupled to a LED was also used to verify the synchronization between the differential pressure signal and the acquired images.

The experimental conditions evaluated in this study were selected to keep the gas and liquid flows within the limits for which the wet gas condition is established based on the Lockhart-Martinelli parameter (X_{LM}), considering the limits of experimental circuit operation. In the context of flow measurement, it is common to limit the wet gas condition to the range of 0-0.3 for the X_{LM} (Campos *et al.*, 2014; Zheng *et al.*, 2016).

Figure 1b shows the superficial velocities evaluated in the experiments, depicted on the flow pattern map of Mandhane *et al.* (1974). The superficial gas velocity (J_g) was determined based on the temperature measured in the experiments and the outlet pressure (atmospheric). Although the flow pattern map indicates that some of the conditions evaluated would be in the transition between the wavy and slug or annular flow, in all experiments, only the wavy flow pattern was identified upstream of the orifice plate.

2.2 Image processing

The method used for image processing in the present work is exemplified in Fig. 2 for an image obtained in the flow in a constant cross-section pipe. The algorithm was implemented in Python, using the functions of the OpenCV library.

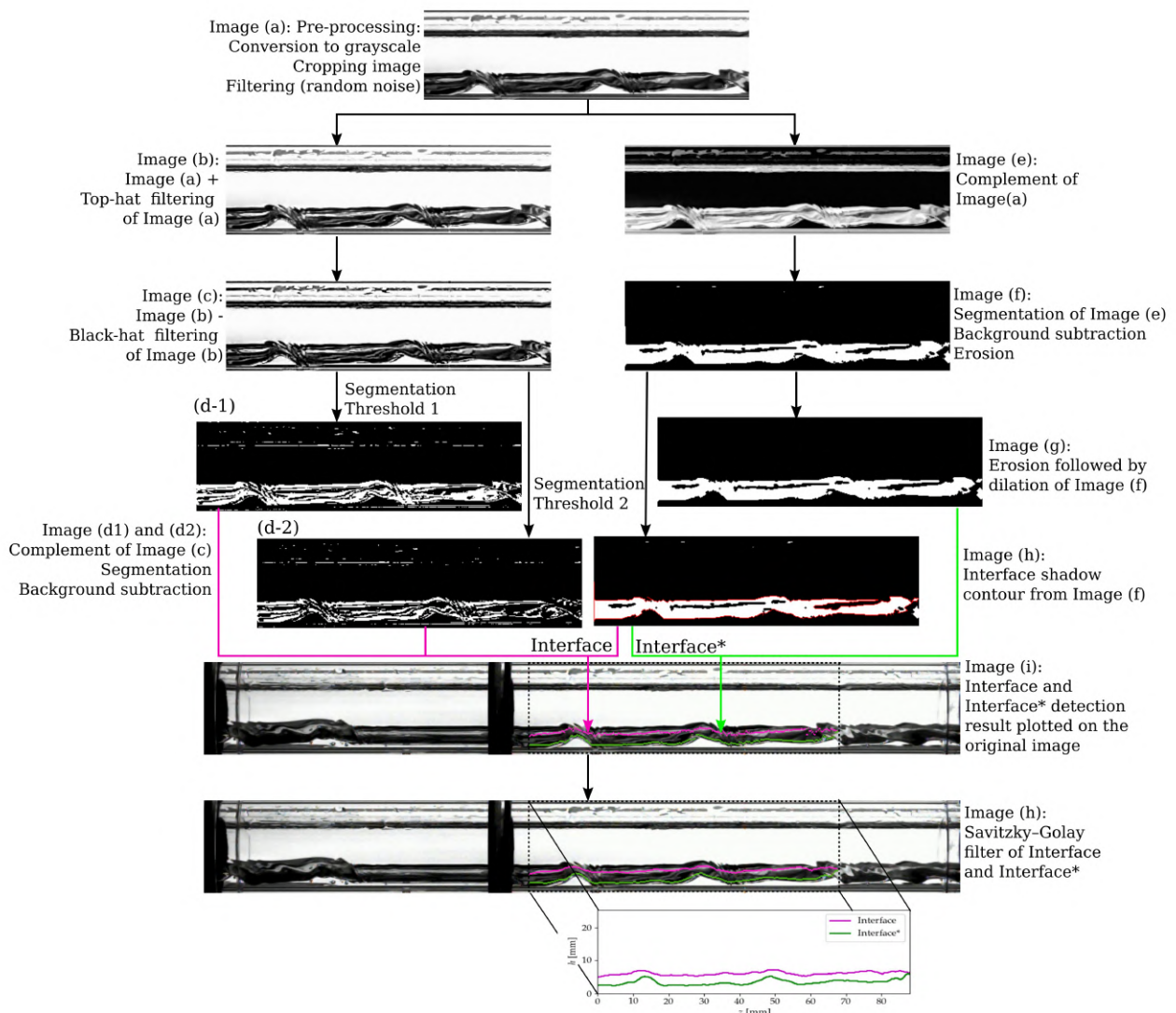


Figure 2. Image processing steps for film height detection.

The image processing steps are based on the steps presented in do Amaral *et al.* (2013) and Hudaya *et al.* (2019) and include the conversion to grayscale, image cropping, image complement, background subtraction, and morphological operations and filters (top hat and black hat), as shown in Fig. 2. In this work, however, the position that best represents the film height appears brighter inside the region shaded by the interface because of the illumination of the visualization section. The gray level of the pixels representing the film height is similar to the gray level observed in the regions where only one phase is present. Therefore, some steps were added to separate the interface region from the image (e, f, h in Fig. 2). Furthermore, when dispersive waves propagate through the test section, a large amount of air bubbles is observed in the liquid, and it is difficult to identify the position of the interface. Thus, in this work, the film height was determined by calculating the average position of pixels with a value below a threshold (d-1 or d-2 in the Fig. 2) within the region characterized as the interface (h in Fig. 2). In addition, the lowest position of the region shaded by the interface, named Interface* was also identified in the images to compare the results of film height fluctuations.

3. RESULTS AND DISCUSSION

The gas-liquid flow through the orifice plate is discussed first in this section based on the analysis of images captured by the HSC to establish the relationship between the flow structures observed in the images and the fluctuations of the DP signal. In Fig. 3 a sequence of images and the DP signal are shown for the experimental condition with $J_g = 10.3$ m/s and $J_l = 0.065$ m/s. For better visualization, the DP signal was treated using a fourth-order digital low-pass Butterworth filter with a frequency of 25 Hz.

In Fig. 3, between the instants t_1 and t_{11} it is possible to observe the propagation of the first wave. When the front of the wave comes into contact with the orifice plate (t_6), there is a significant reduction in the cross-sectional area available for gas flow, and part of the liquid is hindered upstream of the restriction. As the upstream pressure rises, the greater is the force made by the gas to push the liquid through the orifice (between t_6 and t_9). The gas drags the liquid in the form of droplets, forming a two-phase jet in the downstream region. The liquid is not able to completely block the gas flow. The sudden reduction in the cross-sectional area available for gas flow in the orifice implies an increase of the static pressure upstream of the restriction. Therefore, a sudden DP increase is observed in Fig 3b. The partial blockage caused by the liquid decreases as the liquid is pushed through the orifice. Only a few regular waves of small amplitude are observed between the two waves in the region upstream of the orifice plate. This way, the DP decreases, reaching a local minimum in this time interval. From t_{13} onwards, the interface becomes more unstable, and the entrained droplets indicate the approach of the second wave. The wave propagates with a higher velocity than the first one, and its front hits the orifice plate at t_{17} - t_{18} , causing a more abrupt reduction in the cross-sectional area available for gas flow. At this time, it can also be noted how the liquid film in the upper wall of the pipe is dragged into the gas phase core as the front of the wave approaches the restriction, as highlighted in the t_{18} image. The evolution of the liquid concentration downstream of the orifice plate also characterizes the sudden increase (t_{18} to t_{21}) and the reduction (t_{25} to t_{28}) in the liquid flow through the orifice plate. In agreement with the phenomena observed in the images, the amplitude of the DP fluctuation is also higher between t_{12} and t_{28} compared to that observed between t_1 and t_{11} . It can be noticed from the DP signal in Fig. 3b that the analysis is performed in a time interval in which the flow is statistically developed, with the superficial velocities of gas and liquid kept constant at the inlet.

The dependence of the gas and liquid superficial velocities on the flow upstream of the orifice plate is exemplified in Fig. 4, in which the film heights obtained from the image processing are highlighted. The region selected for determining the liquid film height starts at a distance of $2.3 D$ from the orifice plate, with a length of $1.8 D$. A sequence of four images separated by an interval of 20 ms for each experimental condition evaluated is presented.

Regarding the identification of the interface height, it is observed that the liquid film height h_i^{I*} adequately represents the lower position of the area shaded by the interface, without the bubbles in the liquid film having a significant interference in this parameter. Furthermore, from the application of the proposed methodology, the liquid film height h_i^I accurately represents the position of a regular interface, and satisfactory results were obtained when the interface is significantly diffused, as a consequence of the entrainment of one phase into the other.

In Fig. 4 it can be seen that the two liquid superficial velocities evaluated for $J_g = 6.7$ m/s result in very different phase distributions. While for $J_l = 0.033$ m/s, only small instabilities are observed at the interface, for $J_l = 0.065$ m/s, waves of large amplitude are formed and result in a significant blockage in the cross-sectional area available for gas flow. It is evident that, in the latter case, the effect of the interaction of these waves with the orifice plate will predominate over the others in the DP fluctuations. When increasing the superficial velocity of the gas to $J_g = 10.3$ m/s, as discussed based on the Fig. 3, unstable and higher amplitude waves are also observed. Depending on the amount of liquid they carry and their velocity, these waves have different impacts on DP signal fluctuations. Compared to experiments performed with $J_g = 10.3$ m/s, having as reference the same liquid superficial velocity, in experiments with $J_g = 14.0$ m/s, it is observed that the liquid film height decreases, the amplitude of waves is smaller, and the instabilities at the interface increase. In turn, the high velocity of the gas results in the liquid being atomized into smaller droplets in the orifice plate, which are then entrained in the gas core.

After the identification of the film height in each image, the time series of the liquid film height were determined for

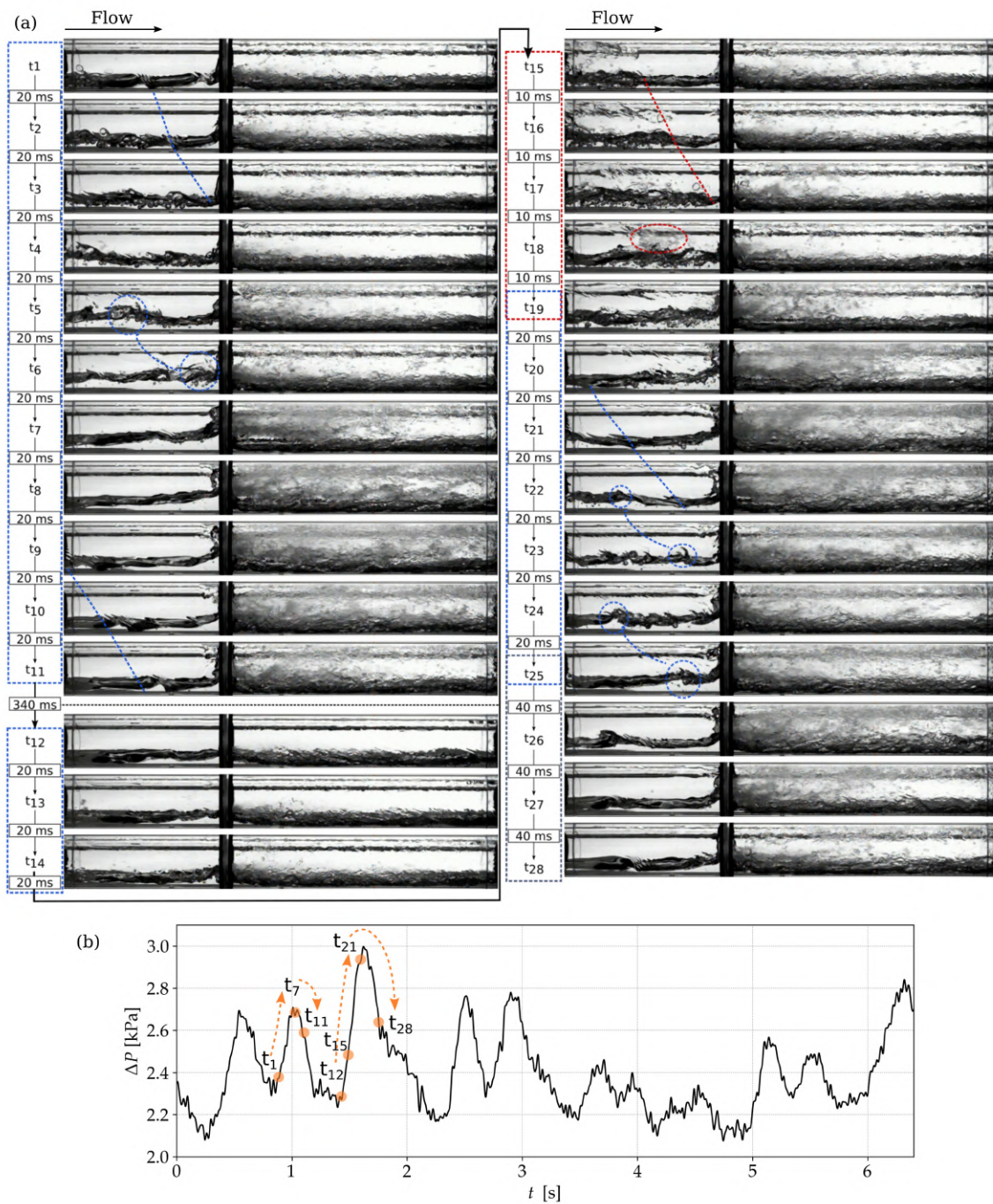


Figure 3. Air-water flow through the orifice plate for $J_g = 10.3$ m/s and $J_l = 0.065$ m/s. (a) Sequence of flow images; (b) Differential pressure signal at orifice plate.

$h_l^I(t)$ and for $h_l^{I^*}(t)$ in monitoring positions predefined along the analysis area. In Fig. 5, for each of the evaluated experimental conditions, the overlap between the time series obtained for the liquid film height upstream of the orifice plate and for the fluctuations of the DP signal across the restriction are shown. As both $h_l^I(t)$ and $h_l^{I^*}(t)$ presented very similar behavior, only the fluctuations of $h_l^I(t)$ are displayed.

From Fig. 5, it is evident that for the evaluated experimental conditions, fluctuations of the DP signal are correlated with the liquid film height fluctuations, which, in turn, are due to the growth and propagation of waves in the flow upstream of the orifice plate. For the experimental conditions evaluated with $J_g = 6.7$ m/s, for the case with $J_l = 0.033$ m/s, both the pressure and the liquid height have small amplitude fluctuations. However, it is still possible to notice the correlation between the variables. For the case with $J_l = 0.065$ m/s, it is evident how fluctuations in the height of the film lead to

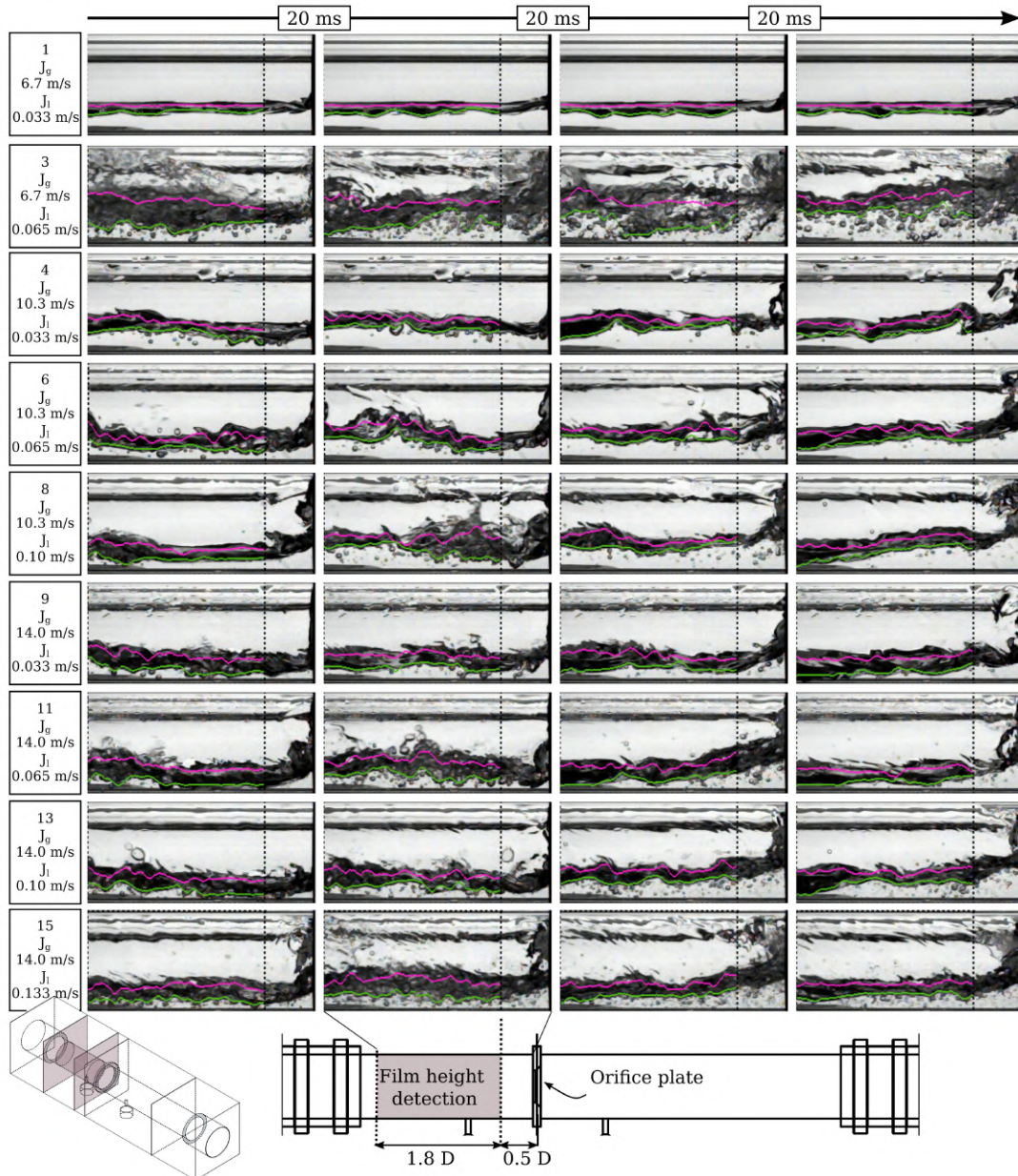


Figure 4. Interface contours obtained for the flow images with the orifice plate. The interval between images is equal to 20 ms.

DP fluctuations. It is noted that the DP fluctuations' amplitude depends not only on the amplitude of the upstream waves but on the combination between the wave amplitude, wavelength, and wave velocity. So the DP fluctuations depend on the liquid volume carried by the wave and will pass through the orifice plate in a certain time interval. As an example, observing the first wave that is identified from $h_l^I(t)$ in Fig. 5 for $J_l = 0.065$ m/s, and comparing its amplitude with the amplitude of the second wave identified in the same case, it is verified that in terms of amplitude the waves are similar. However, the volume of liquid transported is smaller in the first wave by comparing the time interval in which the liquid height remains at a higher level. Therefore, the amplitude of the DP fluctuation is also smaller. It is also observed sudden rise and fall in the height of the liquid film during the passage of a wave, while the pressure gradually decreases after a more sudden rise. It can be associated with the amount of liquid that remains dammed at the edges of the orifice plate.

The observations made about the correlation between the height of the liquid film for the experimental condition with $J_g = 6.7$ m/s and $J_l = 0.065$ m/s, are valid for the other experimental conditions shown in Fig. 5. However, one difference is that a series of successive waves may be associated with a single fluctuation in the DP signal, so the dominant frequencies in the DP signal may not correspond to the dominant frequencies identified for the h_l^I time series. This phenomenon is observed, for example, between 2 and 3 s for experimental condition with $J_g = 10.3$ m/s and $J_l = 0.1$ m/s and for experimental conditions with $J_g = 14$ m/s and $J_l \geq 0.065$ m/s (Fig. 5).

Figure 6 shows the mean and standard deviation of the differential pressure as a function of the Lockhart-Martinelli

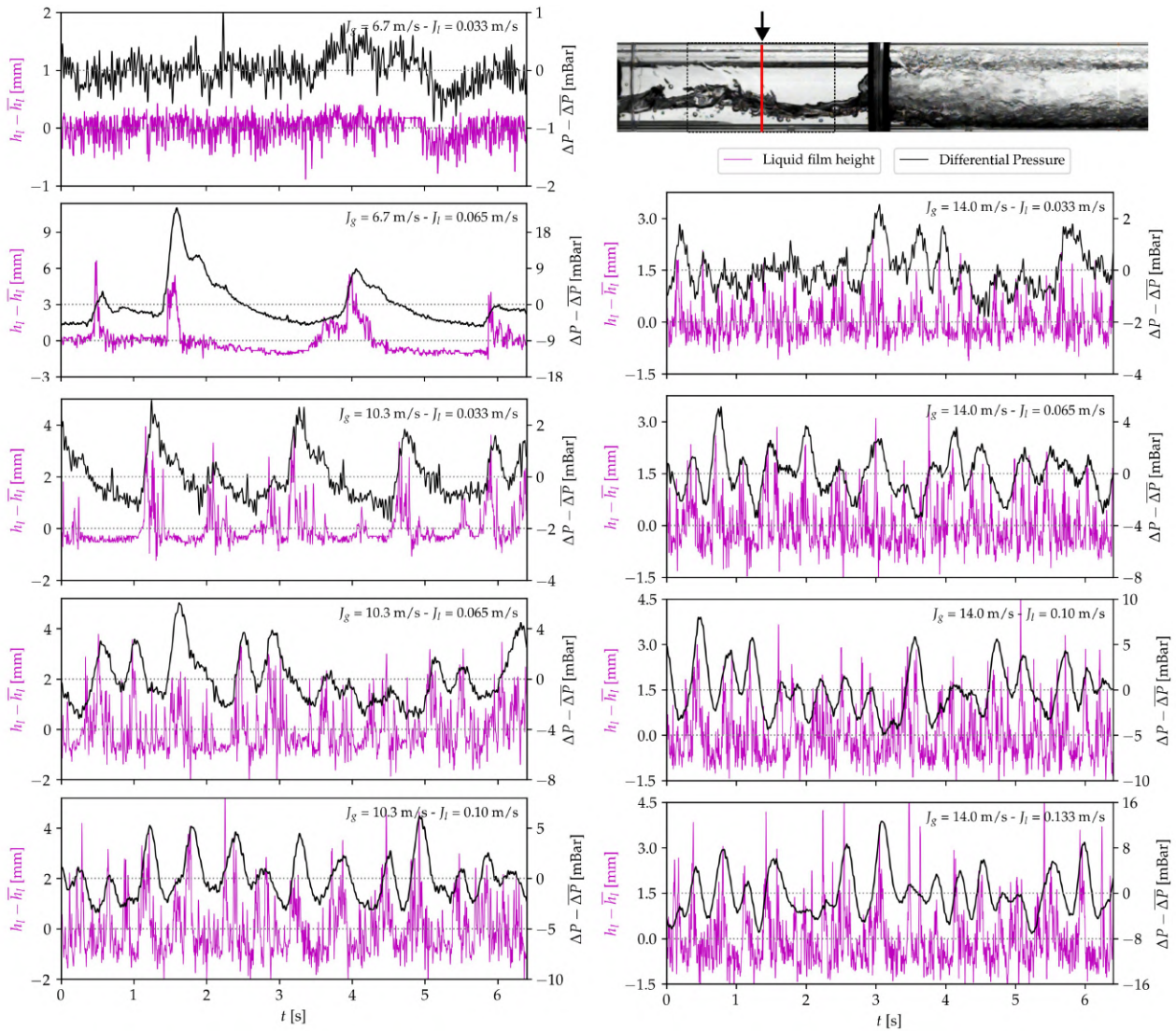


Figure 5. Fluctuations in liquid film height upstream of orifice plate and differential pressure through the orifice plate.

parameter for the different gas superficial velocities evaluated. In addition to the conditions shown in Fig. 1b, some intermediate points between the liquid superficial velocities already reported were also evaluated. For this analysis, the tests were performed with five repetitions for each two-phase experimental condition, with each test corresponding to 120 s of measurement.

Figure 6a shows that the mean DP increases as the gas superficial velocities increase. In agreement with the results presented by Zheng *et al.* (2016), the increase in the gas flow has a higher impact on the mean DP than the increase in the same proportion of the liquid flow rate.

The results obtained for the DP standard deviation are shown in Fig. 6b. The standard deviation increases with the increase of the liquid superficial velocity for a given gas superficial velocity. From the comparison between Fig. 6a and b, a higher dependence of the DP standard deviation than the DP mean with the liquid fraction is observed.

4. CONCLUSIONS

In this work, the wavy stratified flow through an orifice plate and its relationship with the observed DP fluctuations were discussed. It was identified that for the analyzed test envelope, the DP fluctuations depend on the characteristics of the waves in the flow upstream of the orifice plate, which causes a significant instantaneous decrease in the gas flow area, inducing large pulses in the upstream pressure, and so in the DP through the orifice plate. The superficial velocities of the gas and liquid phases impact on the amplitude of the waves, wavelength, and wave velocity. Therefore, DP does indeed carry valuable information about the liquid content in the flow. The mechanisms behind this correlation had not been analyzed from experimental data in previous works. For the experimental conditions evaluated with gas superficial velocities up to 10.3 m/s and liquid superficial velocities up to 0.065 m/s, the frequency and amplitude of the liquid film

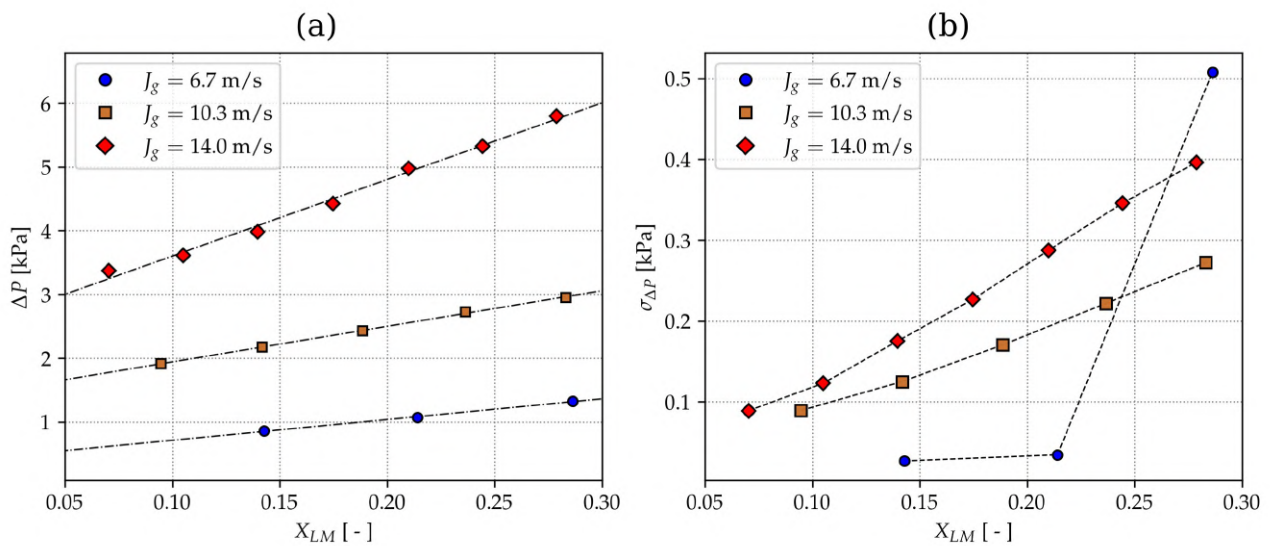


Figure 6. (a) Mean of differential pressure and (b) standard deviation of differential pressure fluctuations through the orifice plate as a function of the Lockhart-Martinelli parameter (X_{LM}).

height fluctuations and DP fluctuations are well correlated. On the other hand, for conditions associated with high gas and liquid superficial velocities, the DP fluctuations may have a characteristic frequency smaller than the liquid film height fluctuations. Therefore, it was not always possible to identify the isolated effect of the passage of each wave through the orifice plate on the DP signal.

Results were also presented for the mean DP through the orifice plate and the standard deviation of the DP fluctuations. The results showed that mean DP has a higher dependence on the gas superficial velocity, while the standard deviation of the fluctuations shows a higher dependence on the liquid fraction.

It is worth mentioning that DP fluctuations are also observed in wavy stratified flow in pipes, which allows characterizing the liquid fraction even without the orifice plate. However, the presence of a restriction amplifies these fluctuations, which can lead to a higher sensitivity in predicting the liquid fraction. The continuity of the research should evaluate the influence of different flow patterns upstream of the orifice plate and the orifice plate diameter ratio on the DP fluctuations from the simultaneous acquisition between the flow images and the DP signal. The results will also compose a database for developing and validating CFD models of multiphase flow through constrictions.

5. ACKNOWLEDGEMENTS

The authors would like to thank to Conselho Nacional de Desenvolvimento Científico e Tecnológico (CNPq, Brazil).

6. REFERENCES

- Almalki, N. and Ahmed, W.H., 2020. "Evaluating the two-phase flow development through orifices using a synchronised multi-channel void fraction sensor". *Experimental Thermal and Fluid Science*, Vol. 118, p. 110165.
- Ayati, A.A., Farias, P.S.C., Azevedo, L.F.A. and de Paula, I.B., 2017. "Characterization of linear interfacial waves in a turbulent gas-liquid pipe flow". *Physics of Fluids*, Vol. 29, No. 6, p. 062106.
- Campos, S.R., Baliño, J.L., Slobodcicov, I., Filho, D.F. and Paz, E.F., 2014. "Orifice plate meter field performance: Formulation and validation in multiphase flow conditions". *Experimental Thermal and Fluid Science*, Vol. 58, pp. 93–104.
- Chisholm, D., 1977. "Two-Phase flow through Sharp-Edged Orifices". *Journal of Mechanical Engineering Science*, Vol. 19, No. 3, pp. 128–130.
- do Amaral, C., Alves, R., da Silva, M., Arruda, L., Dorini, L., Morales, R. and Pipa, D., 2013. "Image processing techniques for high-speed videometry in horizontal two-phase slug flows". *Flow Measurement and Instrumentation*, Vol. 33, pp. 257–264.
- He, D.H. and Bai, B.F., 2014. "Two-phase mass flow coefficient of V-Cone throttle device". *Experimental Thermal and Fluid Science*, Vol. 57, pp. 77–85.
- Hudaya, A.Z., Widyatama, A., Dinaryanto, O., Juwana, W.E., Indarto and Deendarlianto, 2019. "The liquid wave characteristics during the transportation of air-water stratified co-current two-phase flow in a horizontal pipe". *Experimental Thermal and Fluid Science*, Vol. 103, pp. 304–317.

- Kuntoro, H.Y., Hudaya, A.Z., Dinaryanto, O., Majid, A.I. and Deendarlianto, 2016. "An improved algorithm of image processing technique for film thickness measurement in a horizontal stratified gas-liquid two-phase flow". *AIP Conference Proceedings*, Vol. 1737.
- Li, S., Zhao, F., Zheng, X., He, D. and Bai, B., 2020a. "Wet gas metering by cone throttle device with machine learning". *Measurement*, Vol. 164, p. 108080.
- Li, S., Zheng, X., Zhao, F., He, D. and Bai, B., 2020b. "Comparison of throttle devices to measure two-phase flowrates of wet gas with extremely-low liquid loading". *Flow Measurement and Instrumentation*, Vol. 76, p. 101840.
- Lin, Z.H., 1982. "Two-phase flow measurements with sharp-edged orifices". *International Journal of Multiphase Flow*, Vol. 8, No. 6, pp. 683–693.
- Ma, Y., Liu, W., Wu, H., Liu, Y., Lyu, J. and Cai, Z., 2020. "Visualization experiment of gas-liquid flow pattern downstream of single-orifice plates in horizontal pipes under an intermittent upstream flow". *Experimental Thermal and Fluid Science*, Vol. 119, p. 110206.
- Maidana, N.d.C., 2017. *Disturbances induced by an orifice plate on a horizontal air-water flow in the slug regime (in Portuguese)*. Master's thesis, School of Mechanical Engineering, University of Campinas, São Paulo, Brasil.
- Maidana, N.d.C. and Rosa, E.S., 2018. "Flow disturbances induced by an orifice plate in a horizontal air-water flow in the slug regime". *Experimental Thermal and Fluid Science*, Vol. 94, pp. 59–76.
- Mandhane, J.M., Gregory, G.A. and Aziz, K., 1974. "A flow pattern map for gas-liquid flow in horizontal pipes". *International Journal of Multiphase Flow*, Vol. 1, No. 4, pp. 537–553.
- Murdock, J.W., 1962. "Two-Phase Flow Measurement With Orifices". *Journal of Basic Engineering*, Vol. 84, No. 4, pp. 419–432.
- Pan, Y., Hong, Y., Sun, Q., Zheng, Z., Wang, D. and Niu, P., 2019. "A new correlation of wet gas flow for low pressure with a vertically mounted venturi meter". *Flow Measurement and Instrumentation*, Vol. 70, p. 101636.
- Steven, R.N., 2002. "Wet gas metering with a horizontally mounted Venturi meter". *Flow Measurement and Instrumentation*, Vol. 12, No. 5-6, pp. 361–372.
- Wenran, W. and Yunxian, T., 1995. "A new method of two-phase flow measurement by orifice plate differential pressure noise". *Flow Measurement and Instrumentation*, Vol. 6, No. 4, pp. 265–270.
- Widyatama, A., Dinaryanto, O., Indarto and Deendarlianto, 2018. "The development of image processing technique to study the interfacial behavior of air-water slug two-phase flow in horizontal pipes". *Flow Measurement and Instrumentation*, Vol. 59, pp. 168–180.
- Xu, L., Xu, J., Dong, F. and Zhang, T., 2003. "On fluctuation of the dynamic differential pressure signal of Venturi meter for wet gas metering". *Flow Measurement and Instrumentation*, Vol. 14, No. 4-5, pp. 211–217.
- Zheng, X., He, D., Yu, Z. and Bai, B., 2016. "Error analysis of gas and liquid flow rates metering method based on differential pressure in wet gas". *Experimental Thermal and Fluid Science*, Vol. 79, pp. 245–253.

7. RESPONSIBILITY NOTICE

The authors are solely responsible for the printed material included in this paper.